Generic Structure of Multilevel Quantum Beats

C. Leichtle, I. Sh. Averbukh,* and W. P. Schleich†
Abteilung für Quantenphysik, Universität Ulm, D-89069 Ulm, Germany
(Received 29 January 1996)

Many transient signals from quantum systems result from beats among a large number of levels whose energies depend nonlinearly on the quantum number. Typical examples range from time-resolved laser femtochemistry to quantum optics of single atoms in cavities. Starting from rather general assumptions on the nature of the system, we derive approximate closed-form expressions, which describe such signals in the semiclassical limit. Our approach brings out in a most natural way the phenomenon of fractional revivals and full revivals and explains the oscillatory structures observed in recent experiments on atomic wave packets [Phys. Rev. Lett. **72**, 3783 (1994)]. [S0031-9007(96)01607-9]

PACS numbers: 42.50.Md

Time-dependent signals originating from a large number of simultaneously excited quantum levels appear in the physics of wave packets in atoms [1], molecules [2], and cavity QED [3]. Wave packets explore the correspondence principle at the quantum-classical border [4]. Moreover, this field is closely related to laser femtochemistry [5], which studies molecular dynamics and chemical reactions "in real time." Despite the different physical nature of these systems and the studied signals, there is a surprising similarity [6] in the overall structure of their temporal behavior, as exemplified by Fig. 1 for the case of an atomic wave packet. In addition to the universal feature of fractional revivals and full revivals [7–11] in such transient signals, there is also a certain universality in their fine structure as can be seen from Fig. 1(b).

In the present Letter we introduce for the first time an *analytical* approach towards this universal behavior of beat signals. Our analysis describes not only the shapes of individual peaks, but also reproduces properly the behavior of groups of peaks over a wide time range. We emphasize that the long-time limit of such multilevel quantum beats has only recently become experimentally accessible [8].

For time intervals, in which relaxation is negligible, transient signals such as the one of Fig. 1 are generally of the form [10]

$$S(t) = \sum_n P_n e^{i\omega(n)t} = e^{i\omega(\overline{n})t}\mathcal{S}(t) \qquad (1)$$

with

$$\mathcal{S}(t) = \sum_{m=-\infty}^{\infty} P_{\overline{n}+m} \times \exp\left[2\pi i\left(\frac{t}{T_1}m - \frac{t}{T_2}m^2 + \frac{t}{T_3}m^3 + \cdots\right)\right]. \qquad (2)$$

Here we assume that the distribution of weight factors P_n is normalizable, has a dominant maximum at the integer $\overline{n}$ and the width $\Delta n \gg 1$. The characteristic times $T_j = j!\,2\pi/|\omega^{(j)}(\overline{n})|$ follow from the derivatives $\omega^{(j)}$ of the frequencies $\omega(n)$ of the underlying quantum system with respect to n. Note that for definiteness we have chosen the signs of the second and third derivative of ω as in the Coulombic case, where the spectrum reads $E(n) = -R_y/n^2$ with the Rydberg constant $R_y = 13.6$ eV. In the semiclassical limit the natural time scales T_j are well separated and build up a hierarchy $T_1 \ll T_2 \ll T_3 \ll \cdots$.

The temporal behavior of the experimental signal shown in Fig. 1 is not obvious from the *form* of $S(t)$ in Eq. (2). Nevertheless, we can extract the characteristic features by performing an exact transformation of this sum. The key idea of our approach is a decomposition into a number of subsums, each of which contains only terms whose phases are close to each other. We achieve this by combining each rth term of the original sum to one subsum. The particular choice of r depends on the time interval of interest.

Consider, for example, the behavior of $\mathcal{S}(t)$ in the neighborhood of the time $t = q/r\,T_2$ where fractional revivals appear [11]. Here q and r are mutually prime integers. It is advantageous to shift the origin of time into the region of $q/r\ T_2$ and choose it to be an integer multiple l of T_1, that is

$$t \equiv lT_1 + \Delta t \equiv \frac{q}{r}T_2 + \epsilon_{q/r}T_1 + \Delta t\,, \qquad (3)$$

where the remainder $|\epsilon_{q/r}| \leq 1/2$. Hence the sum $\mathcal{S}(\Delta t) \equiv \mathcal{S}(t = q/rT_2 + \epsilon_{q/r}T_1 + \Delta t)$ reads

$$\mathcal{S}(\Delta t) = \sum_{m=-\infty}^{\infty} \gamma_m^{(r)} W_m(\Delta t)\,, \qquad (4)$$

where

$$\gamma_m^{(r)} \equiv \exp\left(-2\pi i\,\frac{q}{r}\,m^2\right) \qquad (5)$$

and

$$W_m(\Delta t) \equiv P_{\overline{n}+m}\exp\left\{2\pi i\left[\frac{\Delta t}{T_1}m - \left(\epsilon_{q/r} + \frac{\Delta t}{T_1}\right)\frac{T_1}{T_2}m^2 + \left(l + \frac{\Delta t}{T_1}\right)\frac{T_1}{T_3}m^3 + \cdots\right]\right\}. \qquad (6)$$

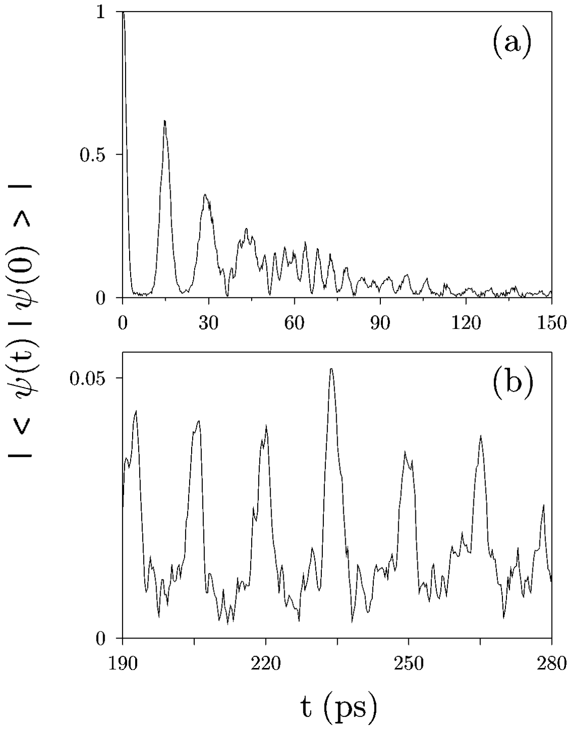

FIG. 1. Experimental data [7] of the autocorrelation function $C(t) = |\langle\psi(t)\,|\,\psi(0)\rangle|$ of an atomic wave packet. From (a) we recognize that in the early stage $C(t)$ is almost periodic with a period $T_1 \simeq 15.3$ ps corresponding to the typical energy separation between neighboring eigenstates. However, for larger times this periodicity disappears and new features emerge: At fractions of another characteristic time $T_2 \gg T_1$ the system is again periodic, a phenomenon referred to as fractional revivals. The period is now a fraction of T_1. In the immediate vicinity of the time $T_2 \simeq 474$ ps the signal would even restore almost completely its initial shape giving rise to full revivals. However, the same periodicity occurs near the time point $T_2/2 \simeq 237$ ps as shown in (b), but in this region the signal pattern is shifted by $T_1/2$ with respect to the initial one. These fractional revivals show an asymmetric shape with a fast decay on one side and a slow oscillatory fall down on the other.

Here we have used that according to Eq. (3) $\exp(2\pi imt/T_1) = \exp(2\pi im\Delta t/T_1)$. Note that this representation of the sum S depends on the choice of the origin of time and thus on the fraction q/r. Hence for every different time region under consideration we adopt a different representation of the sum S.

We proceed by noting that the function $\gamma_m^{(r)}$, Eq. (5), is periodic in m with period r, that is $\gamma_{m+r}^{(r)} = \gamma_m^{(r)}$. In order to make use of this periodicity we rearrange the summation with the help of the relation

$$\sum_{m=-\infty}^{\infty} a_m = \sum_{p=0}^{r-1} \sum_{k=-\infty}^{\infty} a_{p+kr}\,. \tag{7}$$

This technique combines those terms to subsums whose phases are close to each other [12]. Since $\gamma_{p+kr}^{(r)} = \gamma_p^{(r)}$, we find

$$S(\Delta t) = \sum_{p=0}^{r-1} \gamma_p^{(r)} \sum_{k=-\infty}^{\infty} W_{p+kr}(\Delta t)\,. \tag{8}$$

We now apply the Poisson summation formula [13]

$$\sum_{k=-\infty}^{\infty} f_k = \sum_{m=-\infty}^{\infty} \int_{-\infty}^{\infty} dk\, f(k) \exp(-2\pi ikm) \tag{9}$$

to the subsums over k in Eq. (8). This allows us to represent the discrete superposition of many harmonics as a sequence of time dependent signals numbered by the index m and arriving one after another. The application of this formula leads to a significant simplification when the width of each signal in time is shorter than the separation between two signals. Indeed we arrive at

$$S(\Delta t) = \sum_{p=0}^{r-1} \gamma_p^{(r)} \sum_{m=-\infty}^{\infty} \times \int_{-\infty}^{\infty} dk\, W(p + kr, \Delta t) \exp(-2\pi ikm)\,, \tag{10}$$

where $W(x, \Delta t)$ is the continuous version of $W_m(\Delta t)$, Eq. (6). When we introduce the new integration variable $x = p + kr$, the integral over x is independent of p, that is

$$S(\Delta t) = \frac{1}{r} \sum_{p=0}^{r-1} \gamma_p^{(r)} \sum_{m=-\infty}^{\infty} \exp\left(2\pi i\, \frac{p}{r}\, m\right) \times \int_{-\infty}^{\infty} dx\, W(x, \Delta t) \exp\left(-2\pi i\, \frac{m}{r}\, x\right). \tag{11}$$

The interchange of the two summations allows one to write the sum S now in the form

$$S(\Delta t) = \sum_{m=-\infty}^{\infty} \mathcal{W}_m^{(r)} I_m^{(r)}(\Delta t)\,, \tag{12}$$

where

$$\mathcal{W}_m^{(r)} = \frac{1}{r} \sum_{p=0}^{r-1} \exp\left[2\pi i\left(p\, \frac{m}{r} - p^2\, \frac{q}{r}\right)\right] \tag{13}$$

and

$$I_m^{(r)}(\Delta t) = \int_{-\infty}^{\infty} dx\, P(\overline{n} + x) \exp\left\{2\pi i\left[\left(\frac{\Delta t}{T_1} - \frac{m}{r}\right)\right]x - \left(\epsilon_{q/r} + \frac{\Delta t}{T_1}\right)\frac{T_1}{T_2}\, x^2 + \left(l + \frac{\Delta t}{T_1}\right)\frac{T_1}{T_3}\, x^3 + \cdots\right]\right\}. \tag{14}$$

The exact representation of the sum S in Eq. (12) is the central result of the paper. It reveals in the most obvious way the revival structure of the signal S, because each fractional revival corresponds to a single term in the sum Eq. (12). Before we illustrate this feature by discussing the functions $\mathcal{W}_m^{(r)}$ and $I_m^{(r)}(\Delta t)$ in more detail, we note that our method also allows one to investigate the full revivals by setting $q = r = 1$.

The function $\mathcal{W}_m^{(r)}$ is independent of the distribution P_n and the time Δt. Thus it acts in the sum Eq. (12) as a weighting factor. Because of the properties of $\mathcal{W}_m^{(r)}$ discussed in Ref. [11], only every second term in the sum Eq. (12) has a nonvanishing value when r is even, whereas for r odd this is true for every value of m.

Now we turn to the discussion of $I_m^{(r)}(\Delta t)$ and its time dependence. To be specific, we use the example of the Coulombic spectrum together with a Gaussian distribution for P_n. In order to be consistent with the experimental data presented in Fig. 1 we choose for the center $\overline{n}$ and the variance Δn of the Gaussian the numerical values $\overline{n} = 46$ and $\Delta n = 2$. Hence the times T_1 and T_2 take on the values $T_1 \simeq 14.8$ ps and $T_2 = 2\overline{n}T_1/3 = 30.67T_1 \simeq 460$ ps. In Fig. 2(a) we show by a dashed curve the behavior of the modulus of the sum Eq. (1) in the vicinity of $t = \frac{1}{2}T_2$, where the fractional revivals of order $\frac{1}{2}$ occur. Here we have evaluated Eq. (1) numerically. We note that this signal shows very similar features as in Fig. 1(b).

We proceed by evaluating $I_m^{(r)}$ for the Coulombic case. We first note that for times t of the order of T_2 we can neglect the quartic term and all higher order terms in the expansion in Eq. (14). In this case we can evaluate the integral $I_m^{(r)}(\Delta t)$ analytically as shown in Ref. [14], which yields

$$I_m^{(r)}(\Delta t) = e^{i\,\Phi_m(\Delta t)}G(\Delta t)F_m(\Delta t)\mathrm{Ai}[z_m(\Delta t)]\,. \qquad (15)$$

Here the functions $G(\Delta t)$ and $F_m(\Delta t)$ are defined by

$$G(\Delta t) = A\exp\left[-\sigma\left(\epsilon_{q/r} + \frac{\Delta t}{T_1}\right)^2\right] \qquad (16)$$

and

$$F_m(\Delta t) = \exp\left[\mu\left(\frac{\Delta t}{T_1} - \frac{m}{r}\right)\right], \qquad (17)$$

and $\mathrm{Ai}(z)$ denotes the Airy function of complex argument. The quantities $\Phi_m(\Delta t)$, A, σ, and μ are real whereas $z_m(\Delta t)$ is complex. For the explicit expressions of these quantities we refer to Ref. [14].

We are now in the position to understand the location, shape, and fine structure of each fractional revival shown in Fig. 2(a). For the time region $t \sim T_2/2 = 15.33T_1$, Eq. (3) immediately gives the parameters $q = 1$, $r = 2$, $l = 15$, and hence $\epsilon_{1/2} = -0.33$. Hence the weight factor $\mathcal{W}_m^{(2)}$ takes on the values $|\mathcal{W}_{m=2k}^{(2)}| \equiv 0$ and $|\mathcal{W}_{m=2k+1}^{(2)}| \equiv 1$. Moreover, we find according to Ref. [14] $A = 1.98$, $\sigma = 0.15$, and $\mu = 2.94$.

In Fig. 2(a) we show by a solid line the analytical result, Eq. (12), using Eqs. (15)–(17). We find an excellent agreement between the direct numerical evaluation of the sum S, Eq. (1), and the analytical approximation. In Fig. 2(b) we show by a solid curve the single term $|I_{m=1}^{(2)}(\Delta t)|$ in the sum Eq. (12), together with the Gaussian $G(\Delta t)/A$, the exponential $F_{m=1}(\Delta t)$, and

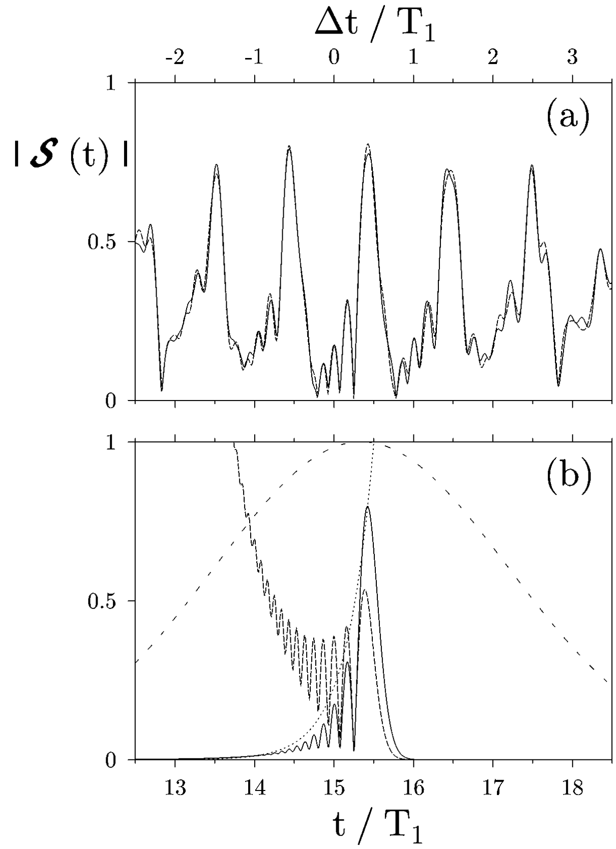

FIG. 2. Fractional revivals of the generic signal $|S(t)|$ for the Coulombic spectrum. In (a) we show by a dashed curve the exact signal Eq. (1) in the neighborhood of $t = \frac{1}{2}T_2 = 15.33T_1$. The solid line shows the signal using the analytical result Eq. (12). We indicate on the top of the figure the relative time Δt introduced in Eq. (3). In (b) we show by a solid line the term $|I_{m=1}^{(2)}(\Delta t)|$, Eq. (15), of the sum Eq. (12). The Gaussian $G(\Delta t)/A$, Eq. (16), the exponential $F_{m=1}(\Delta t)$, Eq. (17), and the absolute value $|\mathrm{Ai}(z_{m=1}(\Delta t))|$ of the complex-valued Airy function are depicted by the dashed, dotted, and broken lines, respectively.

$|\mathrm{Ai}(z_{m=1}(\Delta t))|$. It is the product of the latter two functions, which yields the pronounced peak of $|I_{m=1}^{(2)}(\Delta t)|$ centered at $\Delta t = 0.5T_1$. The Gaussian, which is independent of the index m and centered at $\Delta t = -\epsilon_{1/2}T_1 = 0.33T_1$, just influences the height of the peak, since this function varies very slowly compared to the other two functions. Note that the fine structure of the peak, that is the oscillating structure on its left wing, results exclusively from the Airy function. Figure 2(b) clearly shows that the term $|I_{m=1}^{(2)}(\Delta t)|$ reproduces the fractional revival centered at $t = 15.5T_1$, that is at $\Delta t = 0.5T_1$. Hence there is a one-to-one correspondence between this signal peak and a single term in the sum Eq. (12) [15]. Moreover, the detailed analysis of Ref. [14] shows that a larger value of $|m|$ results in a broader fractional revival centered at $\Delta t_m = m/r\, T_1$ with less pronounced oscillations. This is consistent both with the numerical example of Fig. 2(a) and the experimental data of Fig. 1(a).

When two functions $I_m^{(r)}(\Delta t)$ and $I_{m'}^{(r)}(\Delta t)$ overlap considerably, interferences between these terms in Eq. (12) arise. Then the function $\exp[i\Phi_m(\Delta t)]$ and the phase of the complex Airy function start to play an important role. Consequently, the sum S exhibits a more complicated pattern at the edges of the time window shown in Figs. 1(b) and 2(a). In this regime there is no simple one-to-one correspondence between individual terms in the sum S and the pattern. Nevertheless, Eq. (12) still gives a complete description of the signal S in the vicinity of Δt_m by taking into account only a few terms.

We conclude by noting that the asymmetric oscillations apparent in Fig. 2(b) are a universal feature of transient signals in the long-time limit. They originate from the Airy function which emerges in the most natural way from our theory. The small "forerunner" preceding the main wave packet observed experimentally and explained only numerically in Ref. [7] stems from this Airy function. We can therefore consider this forerunner as a manifestation of "rainbow scattering in the time domain" [16].

In summary, we have presented analytical expressions which describe the generic structure of signals originating from a large number of simultaneously excited quantum levels. A new representation of the underlying sum allowed us for the first time to treat analytically the influence of higher order dispersion effects on quantum beats. The influence of the third order term has already been observed in Ref. [7] in atomic wave packets. The experimental tools in this field have become so refined that even higher order corrections included in our treatment will soon be observed. Moreover, the recent experimental realization of the Jaynes-Cummings model [9] describing the motion of an ion in a Paul trap provides another arena for probing generic structures in the long-time limit of quantum beats.

We enjoyed many stimulating discussions with V. M. Akulin, M. V. Berry, and M. Nauenberg, and thank H. B. van Linden van den Heuvell and J. Wals for many fruitful conversations and for providing us with the experimental data shown in Fig. 1. One of us (I. A.) appreciates the kind hospitality and support at the Universität Ulm. C. L. thanks the Deutsche Forschungsgemeinschaft for its support and acknowledges the warm hospitality during his stay at the Weizmann Institute of Science, Rehovot.

*Also Weizmann Institute of Science, Rehovot, 76100, Israel.
†Also Max-Planck-Institut für Quantenoptik, D-85748 Garching, Germany.

[1] For a review, see, e.g., G. Alber and P. Zoller, Phys. Rep. **199**, 231 (1990).
[2] For a review, see, e.g., M. Gruebele and A. Zewail, Phys. Today **43**, 24 (1990); B. M. Garraway and K.-A. Suominen, Rep. Prog. Phys. **58**, 365 (1995).
[3] J. H. Eberly *et al.*, Phys. Rev. Lett. **44**, 1323 (1980).
[4] M. Nauenberg *et al.*, Sci. Am. **270**, No. 6, 24 (1994), and references therein; M. Nauenberg, Comments At. Mol. Phys. **25**, 151 (1990).
[5] A. H. Zewail, *Femtochemistry* (World Scientific, Singapore, 1994), Vols. 1 and 2.
[6] General aspects of the dynamics of wave packets in atomic, molecular, and quantum optical systems are discussed in a review article by I. Sh. Averbukh and N. F. Perel'man, Sov. Phys. Usp. **34**, 572 (1991).
[7] J. Wals *et al.*, Phys. Rev. Lett. **72**, 3783 (1994); J. Wals *et al.*, Physica Scr. **T58**, 62 (1995).
[8] For the experimental observation of fractional revivals and full revivals of atomic wave packets, see, e.g., J. A. Yeazell *et al.*, Phys. Rev. Lett. **64**, 2007 (1990); J. A. Yeazell and C. R. Stroud, Jr., Phys. Rev. A **43**, 5153 (1991); D. R. Meacher *et al.*, J. Phys. B **24**, L63 (1991); L. Marmet *et al.*, Phys. Rev. Lett. **72**, 3779 (1994); G. Raithel *et al.*, J. Phys. B **27**, 2849 (1994). For molecular wave packets, see T. Baumert *et al.*, Chem. Phys. Lett. **191**, 639 (1992); I. Fischer *et al.*, J. Chem. Phys. **102**, 5566 (1995); M. J. J. Vrakking *et al.*, Phys. Rev. A **54**, R37 (1996).
[9] For the experimental observation of "Jaynes-Cummings (J-C) revivals" in cavity QED, see G. Rempe *et al.*, Phys. Rev. Lett. **58**, 353 (1987); M. Brune *et al.*, Phys. Rev. Lett. **76**, 1800 (1996); in Paul traps, see D. M. Meekhof *et al.*, Phys. Rev. Lett. **76**, 1796 (1996). Note, however, that these "J-C revivals" are a short-time phenomenon and occur at integer multiples of T_1. They therefore correspond to the T_1-periodic behavior of the autocorrelation function of Fig. 1(a). In contrast, the revivals as defined in Refs. [7,8,10,11] occur at $T_2 \gg T_1$ and have not yet been observed experimentally for the Jaynes-Cummings model.
[10] J. Parker and C. R. Stroud, Jr., Phys. Rev. Lett. **56**, 716 (1986).
[11] I. Sh. Averbukh and N. F. Perel'man, Phys. Lett. A **139**, 449 (1989); Sov. Phys. JETP **69**, 464 (1989).
[12] This technique has also been used to treat the integer, fractional, and fractal Talbot effect, see M. V. Berry, J. Phys. A (to be published); M. V. Berry and S. Klein, J. Mod. Optics (to be published); see also J. T. Winthrop and C. R. Worthington, J. Opt. Soc. Am. **49**, 372 (1965).
[13] R. Courant and D. Hilbert, *Methods of Mathematical Physics* (Interscience Publishers, New York, 1953).
[14] C. Leichtle *et al.*, Phys. Rev. A (to be published).
[15] This fact may be used to extract the local parameters of the spectrum by fitting Eq. (15) to experimental data of a *single* (fractional) revival.
[16] For rainbow scattering, see, for example, M. V. Berry and K. E. Mount, Rep. Prog. Phys. **35**, 315 (1972).